ISSN 1062-8738, Bulletin of the Russian Academy of Sciences. Physics, 2013, Vol. 77, No. 9, pp. 1147–1150. © Allerton Press, Inc., 2013.
Original Russian Text © S.B. Erenburg, S.V. Trubina, K.S. Zhuravlev, T.V. Malin, B. Pecz, 2013, published in Izvestiya Rossiiskoi Akademii Nauk. Seriya Fizicheskaya, 2013, Vol. 77, No. 9, pp. 1312–1316.

Diffusion and Deformations in Heterosystems with GaN/AlN Superlattices, According to Data from EXAFS Spectroscopy

S. B. Erenburg[a], S. V. Trubina[a], K. S. Zhuravlev[b], T. V. Malin[b], and B. Pecz[c]

[a] *Institute of Inorganic Chemistry, Siberian Branch, Russian Academy of Sciences, Novosibirsk, 630090 Russia*
[b] *Institute of Semiconductor Physics, Siberian Branch, Russian Academy of Sciences, Novosibirsk, 630090 Russia*
[c] *Research Institute for Technical Physics and Material Science, Hungarian Academy of Sciences, 1121 Budapest, Hungary*
e-mail: simon@niic.nsc.ru

Abstract—Multilayered samples with extremely narrow GaN quantum wells in an AlN host are synthesized via ammonia MBE. The parameters of the microstructure are determined by means of EXAFS spectroscopy, high-resolution electron microscopy, and low-angle scattering. Their relationship to the morphology of GaN/AlN superlattices is established. The influence of growth conditions and the thickness of superlattices on their optical properties and mixing in the near-boundary layers is established.

DOI: 10.3103/S1062873813090116

INTRODUCTION

One promising way of increasing the speed and volume of transmitted information is to move to optical methods of generating, detecting, and recording signals. This requires the development of effective and high-speed photon devices equipped with photodetectors and radiation modulators operating at wavelengths in the near-IR and mid-IR spectral ranges. Such devices are needed to develop terabit fiber-optics communications; for terrestrial communication with air and space vehicles; and for recording the radiation dynamics of atomic, molecular, and solid-state systems. Such functional optical elements can be used in various chemical and biological sensors used to develop devices for analyzing environmental contamination, detecting chemical and biological weapons, conducting medical diagnostics and forensic medicine, and controlling production processes.

GaN-based heterostructures are promising for the development of high-speed terahertz photonic devices, due to the very strong electron–phonon interaction in these strongly ionic materials, which ensures femtosecond restoration times of the initial state. This is an order of magnitude faster than for other semiconductors. Diodes that emit blue light [1], multi-quantum well laser diodes [2], and high-speed field-effect transistors [3] have already been fabricated on the basis of these structures. These are promising for the development of highly sensitive sensors [4]. The large band discontinuity in the conduction band of GaN/AlGaN heterostructures reaches 2 eV for a GaN/AlN heteropair (a record for semiconductor heterostructures), enabling us to design electrooptical switches and photodetectors based on intersubband electron transitions in quantum wells or quantum dots for the mid-IR and near-IR spectral ranges up to 1.3 μm.

Developers have now acquired many years of experience in creating low-dimensional heterostructures based on materials of the A_3B_5 type via molecular beam epitaxy (MBE). The authors of this work also made a considerable contribution to the study of their structural, electron, and optical properties in [5–12].

EXPERIMENTAL

Multilayered samples with extremely narrow GaN quantum wells in an AlN host were synthesized by MBE with ammonia as the source of active nitrogen in order to investigate the influence of growth conditions, thickness, and the number of GaN and AlN layers on stresses and their relaxation in multilayered heterosystems, on the structure of the heterointerfaces in quantum wells, and on the electron and optical spectra of the investigated systems.

An AlN buffer layer 150–500 nm thick was grown on sapphire at a substrate temperature of 1000°C and an ammonia flow rate of 25 st cm^3 min^{-1}. GaN/AlN superlattices were formed on the surface of the AlN layer at a substrate temperature of 830°C and an ammonia flow rate of 200 st cm^3 min^{-1}. The thickness of the GaN and AlN layers varied from 1 to 4 nm according to time of exposure, with the number of layers in the sandwich ranging from 20 to 300.

The influence of the diffusion processes at heterointerfaces and the elastic stresses in the structure on the epitaxial growth and properties of the synthesized systems was investigated by means of extended X-ray

Structural parameters found from the GaK $k^2\chi(k)$ EXAFS data ($\Delta k = 2.5–12$ Å^{-1}), Fourier-filtered in the range of 1.0–3.3 Å for bulk (film ~ 1 μm thick) GaN and GaN/AlN superlattices with different numbers of GaN layers (n) and various thicknesses (D) of the superlattices

No.	Thickness of the GaN/AlN layer	Σ of thickness n; D, nm	$N_{Ga} \pm 0.3$	N_{Al}	R(N) ± 0.01 Å	R(Ga) ± 0.01 Å	R(Al) ± 0.03 Å	$2\sigma^2$ (N), Å^2	$2\sigma^2$ (Ga, Al), Å^2	*Fit*
1	4.1/1.5	130; 728	9.9	2.1	1.95	3.18	3.25	0.003	0.018	2.1
2	2.8/1.5	130; 559	9.7	2.3	1.95	3.19	3.26	0.004	0.020	2.6
3	2.6/1.5	173; 709	9.8	2.2	1.96	3.19	3.26	0.004	0.019	2.3
4	2.1/1.1	260; 832	9.7	2.3	1.96	3.19	3.25	0.003	0.021	2.1
5	1.4/2.8	20; 84	9.3	2.6	1.95	3.16	3.13	0.008	0.015	2.9
6	1.7/2.8	20; 90	9.0	3.0	1.95	3.17	3.15	0.013	0.017	5.0
7	1.7/2.8	22; 99	10.6	1.4	1.95	3.18	3.150	0.009	0.014	3.3
8	1.7/2.8	32; 144	10.6	1.4	1.95	3.17	3.150	0.009	0.013	2.9
Thick film	1 μm		11.9		1.97	3.20		0.014	0.018	1.9

R(N); R(Ga), and R(Al) are the Ga–N, Ga–Ga, and Ga–Al interatomic distances, respectively; $2\sigma(N)^2$ and $2\sigma(Ga, Al)^2$ are the Debye–Waller factors for these bonds ($2\sigma^2(Ga) = 2\sigma^2(Al)$); and *Fit* is an index characterizing the divergence between the experimental and model spectra, observed in the course of refining the model parameters (the mismatch parameter).

absorption fine structure (EXAFS) spectroscopy, high-resolution transmission electron microscopy (HRTEM), small-angle X-ray diffraction (SAXRD), and luminescence measurements. The final aim of our study was to establish the optimum synthesis conditions ensuring the two-dimensional growth of layers and the building of superlattices with the required optical properties.

Low-angle scattering was measured on the anomalous scattering station at the Siberian Center for Collective Use of Synchrotron Radiation at the Budker Institute of Nuclear Physics, Siberian Branch, Russian Academy of Sciences, using a synchrotron radiation beam with $\lambda = 0.15396$ nm.

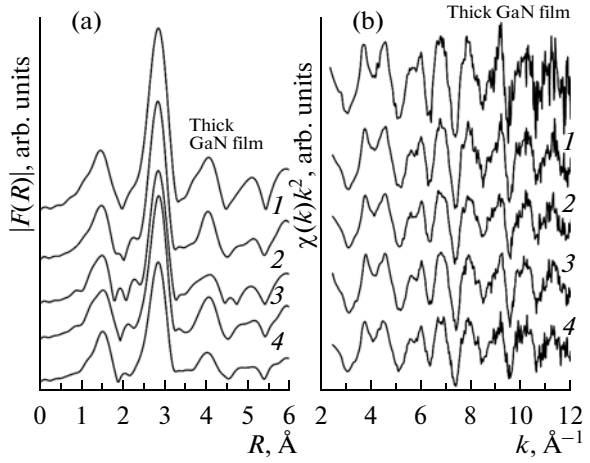

Fig. 1. Modules of the Fourier transform $|F(R)|$ of function $k^2\chi(k)$ GaK EXAFS not including (a) the phase shift and (b) normalized oscillating parts of the GaK EXAFS absorption spectra $k^2\chi(k)$ for samples *1–4* and bulk GaN (thick film).

Electron microphotographs were obtained using a Philips CM20 transmission electron microscope with an electron energy of 200 keV; the samples were treated by ion etching (Ar^+) in an energy range of 3–10 keV.

Luminescence spectra were excited by laser radiation with $E_l = 4.66$ eV ($E_{GaN} = 3.5$ eV $< E_l < 6.2$ eV $= E_{AlN}$, where E_{GaN} and E_{AlN} are the band gaps for GaN and AlN, respectively).

The GaK EXAFS spectra for the heterostructures with the quantum wells were measured using a synchrotron radiation of the VEPP-3 storage ring at the Budker Institute of Nuclear Physics. When recording the spectra, we used the fluorescent procedure for measuring X-ray absorption spectra, which is very sensitive when measuring surface layers. To optimize the measurement process and the subsequent processing of the EXAFS spectra, the samples were arranged at a small (~4°) angle to the incident SR beam, and the table containing the sample was rotated with a frequency of ~15 Hz.

The obtained data were processed using the EXCURV [13] and VIPER10.17 [14] software packages. When processing the data, the phase and amplitude characteristics were calculated in the Xα-DW approximation. The microstructural characteristics (interatomic distances, partial coordination numbers, and Debye–Waller factors) were determined by simulating the experimental spectra (EXAFS fitting). The error in determining the interatomic distances for the first surrounding sphere of an absorbing atom was ≤0.01 Å (≤0.5%).

RESULTS AND DISCUSSION

Figure 1 shows the modules of the Fourier transform $|F(R)|$ of function $k^2\chi(k)$ GaK EXAFS and the normalized oscillating parts of the GaK EXAFS absorption spectra $k^2\chi(k)$ for samples *1–4* and the

bulk GaN (the thick film). The thicknesses of the GaN and AlN films was determined from an analysis of the HRTEM data and are presented in the table. A characteristic TEM microphotograph for one sample (sample *1*) is presented in Fig. 2. During simulation, we determined the factor of amplitude damping $S_0^2 = 1.0$ due to multielectron effects; coordination numbers N_N(Ga–N) = 4; and the sum of coordination numbers N_{Ga}(Ga–Ga) and N_{Al}(Ga–Al) of the second coordination sphere $N_{Ga} + N_{Al} = 12$. The conventional energy of the Fermi level ($E_0 = -8.5$ eV) was determined for bulk GaN and fixed in simulating structures with superlattices. It can be seen from the table that for the multilayered samples with thick (550–850 nm) superlattices ($n = 130–260$), there was minimal shortening (~0.01 Å) of the interatomic Ga–Ga distances R(Ga) relative to the thick film (1 μm), which agreed with the numerous dislocations and the corresponding stress relaxation in the GaN layers found for them. It should be noted that the Ga–Al distance (R(Al)) for the samples with thick superlattices were anomalously long. These distances were ~0.1 Å longer than those characteristic of the Ga–Al solid solutions. It can be seen from the HRTEM microphotographs that the GaN/AlN phase interface is quite pronounced and we cannot speak about the formation of solid solutions in this case. This effect can be explained by the nonequilibrium transition from the growth of GaN to the deposition of AlN, the substantial stresses at the interface, and the relaxation during the growth of thick superlattices. We note that the deposition temperature of both GaN and AlN was ~830°C (see above), substantially lower than was needed to form the equilibrium AlN layer (see above). We assume, however, that this conclusion requires confirmation and more detailed explanation.

The interatomic Ga–Ga distances R(Ga) for samples with fewer layers ($n = 20–32$) and thin (80–150 nm) superlattices fall more substantially (by ~0.03 Å), corresponding to greater deformations and stresses, according to the results obtained earlier for GaN quantum dots in an AlN host [7–9].

Using the known geometry of the atomic arrangement in GaN and AlN crystal lattices, the average coordination numbers of Ga(N_{Ga}) and Al(N_{Al}) for the GaN layers, and the thicknesses of the GaN layers, we performed simple model calculations that allowed us to estimate the degree of Ga and Al mixing in the near-boundary layer for the samples under study. We found the dependences of the N_{Ga}(Ga–Ga) coordination numbers on the number of Ga layers in the GaN films (n) (or the thickness of the GaN films) with different Ga and Al mixing in the boundary GaN layers. The N_{Ga}(Ga–Ga) coordination numbers and thicknesses of the GaN films were determined from an analysis of the EXAFS and HRTEM data, respectively (see table). We thus established that the N_{Ga}(Ga–Ga) ~10.6 coordination numbers for thin samples 7 and 8 (table) corresponded to minor mixing of Ga and Al in the near-boundary layers (≤10%). For thin samples 5 and 6, the N_{Ga} values were somewhat lower (9.3 and 9.0, respectively). Our model estimates found there was more substantial mixing of Ga and Al at the interfaces (~20–30%) in the boundary layers of these samples, due apparently to certain differences in the preliminary treatment of samples 5, 6 and 7, 8. The estimates for thick samples showed more substantial mixing in the boundary layer (~40–50%), due possibly to their multiple heating during preparation.

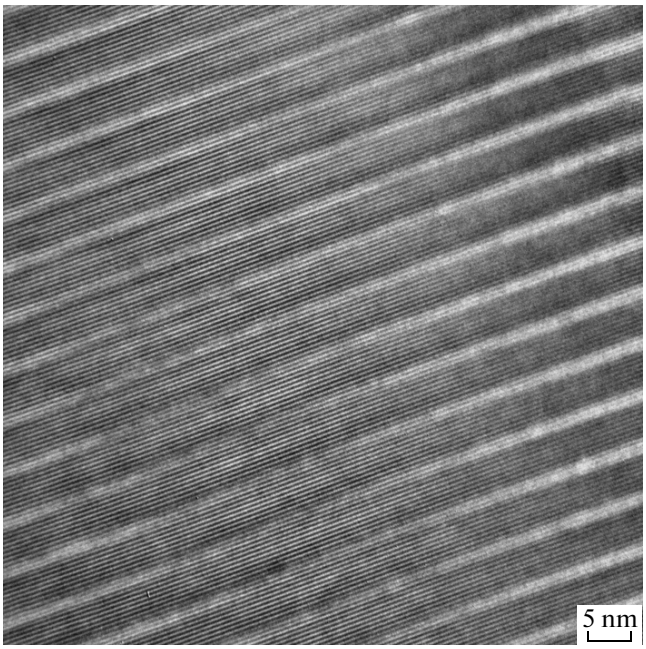

Fig. 2. HRTEM photograph of the superlattice of sample *1*.

It follows from our analysis of features of the luminescence spectra for thin samples that the more intense maxima shifted toward shorter wavelengths were characteristic of samples with more noticeable mixing at the interface (samples 5 and 6 compared to samples 7 and 8; table). It thus seems likely that a certain correlation between the microstructural and optical parameters exists for such samples.

We may conclude from our analysis of the X-ray diffraction pattern on the GaN/AlN superlattice of sample *1* (Fig. 3) that there was no exact correspondence between the location of the maxima and the integer values (n) of the reflection orders predicted according to the Bragg formula ($n\lambda = 2d\sin\theta$, d is the lattice constant). One way of explaining this disagreement is that there were two or more superlattices with close parameters in a sample. If we examine the superlattice period (d) in the low-angle region (up to 9°), then $d_1 = 0.154/2\sin(1.51°/2) \approx 5.8$ nm. At high angles, an additional periodic structure appears that differs from the main structure by ~1.51°/15° = ~0.1 (~10%); i.e., a lattice with d_2 = ~5.8/1.1 = ~5.3 nm is evidently present in the sample.

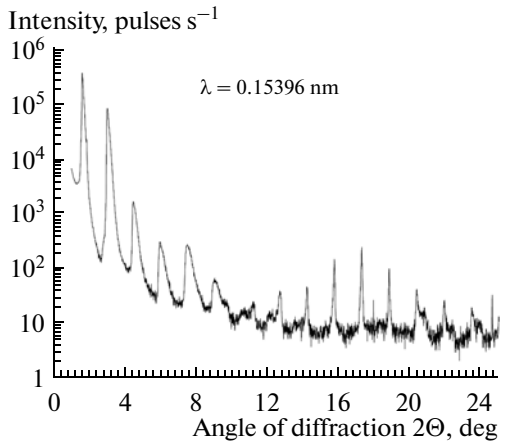

Fig. 3. X-ray diffraction pattern for the GaN/AlN superlattice of sample 1.

The thickness of the GaN and AlN layers found by analyzing the electron microphotographs for sample *1* included 8 and 3 lattice constants (8*c* and 3*c*, c = 0.51 nm for GaN and c = 0.49 nm for AlN), respectively, i.e., ≈4.1 nm and ≈1.5 nm, while lattice constant $d \approx 5.6$ nm. These values are very close to those determined by low-angle diffraction (5.8 and 5.3 nm). The notably different thicknesses of the GaN and AlN layers were determined from microphotographs of sample *3* in its different surface regions (1) and (2): GaN was 7*c* and AlN was 3*c* for (1), while GaN was 5*c* and AlN was 3*c* for (2); i.e., GaN ≈ 3.6 nm and AlN ≈ 1.5 nm for (1), and GaN ≈ 2.6 nm and AlN ≈ 1.5 nm for (2). The superlattice periods (d) were thus $d_1 \approx$ 5.1 nm for (1) and $d_2 \approx 4.1$ nm for (2). The second value of d was very close to the additional value determined from the Raman scattering spectra for this sample ($d \approx 4.3$ nm) and was apparently obtained from a very close surface region.

CONCLUSIONS

Microstructural parameters (interatomic distances, coordination numbers, and Debye–Waller factors) were determined by means of EXAFS spectroscopy, and the relationship between the variations in these parameters and the morphology of superlattices was established.

A minimal drop (~0.01 Å) in the interatomic Ga–Ga distances R(Ga) relative to a thick film was observed for multilayered GaN/AlN samples with thick (550–850 nm) superlattices, agreeing with the numerous dislocations found in them and the corresponding stress relaxation in the GaN layers.

The interatomic Ga–Ga distances R(Ga) for samples with fewer layers and thin (80–150 nm) superlattices fell more substantially (by ~0.03 Å), corresponding to the more substantial deformations and stresses indicated by our earlier results for GaN quantum dots in a AlN host [7–9].

The influence of the growth conditions and the thickness of the superlattices on mixing in the near-boundary layers and the optical properties of the GaN/AlN superlattices was revealed. It was established that Ga–Al mixing occurs only in the layer nearest to the interface.

Anomalously long Ga–Al distances (~3.25 Å) were observed for samples with thick superlattices. This effect can be explained by a nonequilibrium transition from GaN growth to AlN growth and the more substantial stresses at the interface that are apparently characteristic of the growth of such superlattices, and requires confirmation and more detailed explanation.

ACKNOWLEDMGENTS

The authors thank A. Shmakov for participating in our experiment and discussing the results.

This study was performed using the equipment at the Center for Collective Use, Siberian Center for Synchrotron and Terahertz Radiation. It was supported by the RF Ministry of Education and Science; by the Program for Basic Research of the Presidium of the Russian Academy of Sciences, project nos. 24 and 69; and by the Russian Foundation for Basic Research, project no. 12-02-00930.

REFERENCES

1. Nakamura, S., Senoh, M., Nagahama, S., et al., *Jpn. J. Appl. Phys.*, 1996, pt. 2, vol. 1, no. 35, p. L74.
2. Korakakis, D., Ludwig, K.F., and Moustakas, T.D., *Appl. Phys. Lett.,* 1998, vol. 72, no. 9, p. 1004.
3. Wu, Y.-F., Keller, B.P., Kapolnek, D., et al., *Appl. Phys. Lett.*, 1996, vol. 69, no. 10, p. 1438.
4. Gaska, R., Bykhovski, A.D., Shur, M.S., et al., *J. Appl. Phys.*, 1999, vol. 85, no. 9, p. 6932.
5. Mansurov, V.G., Nikitin, A.Yu., Galitsyn, Yu.G., et al., *J. Cryst. Growth*, 2007, vol. 300, no. 1, p. 145.
6. Zhuravlev, K.S., Mansurov, V.G., Protasov, D.Yu., et al., *J. Appl. Phys.*, 2009, vol. 105, no. 11, p. 113712.
7. Erenburg, S.B., Bausk, N.V., Bausk, V.E., et al., *J. Phys.: Conf. Ser.*, 2006, vol. 41, p. 261.
8. Erenburg, S.B., Bausk, N.V., Mazalov, L.N., et al., *Nucl. Instr. Meth. Phys. A,* 2005, vol. 543, no. 1, p. 188.
9. Erenburg, S.B., Trubina, S.V., Bausk, N.V., et al., *J. Phys: Conf. Ser.*, 2009, vol. 190, p. 012131.
10. Aleksandrov, I. and Zhuravlev, K., *Phys. Status Solidi C*, 2010, vol. 7, nos. 7–8, p. 2230.
11. Tronc, P., Zhuravlev, K.S., Mansurov, V.G., et al., *Phys. Rev. B*, 2008, vol. 77, no. 16, p. 165328.
12. Zhuravlev, K.S., Mansurov, V.G., Grinyaev, S.N., et al., *Opt. Zh.*, 2009, vol. 76, no. 12, p. 74.
13. Binsted, N., Campbell, J.W., Gurman, S.J., and Stephenson, P.C., *SERC Daresbury Laboratory Rep.*, 1991.
14. Klementiev, K.V., VIPER for Windows, Freeware.

Translated by N. Korovin